

## A new approach to scatter correction in SPECT images based on Klein\_Nishina equation

Mohsen Hajizadeh Saffar<sup>1</sup>, Shabnam Oloomi<sup>2</sup>, Peter Knoll<sup>3</sup>, Hadi Taleshi<sup>4</sup>

<sup>1</sup>Medical Physics Research Center, School of Medicine, Mashhad University of Medical Sciences, Mashhad, Iran

<sup>2</sup>Medical Physics Department, Mashhad University of Medical Science, Mashhad, Iran

<sup>3</sup>Department of Nuclear Medicine, Wilhelminenspital, Vienna, Austria

<sup>4</sup>Department of Medical Physics, Faculty of Medical Sciences, Tarbiat Modares University, Tehran, Iran

(Received 19 November 2012, Revised 1 April 2013, Accepted 7 April 2013)

### ABSTRACT

**Introduction:** Scattered photon is one of the main defects that degrade the quality and quantitative accuracy of nuclear medicine images. Accurate estimation of scatter in projection data of SPECT is computationally extremely demanding for activity distribution in uniform and non-uniform dense media.

**Methods:** The objective of this paper is to develop and validate a scatter correction technique that use an accurate analytical model based on Klein\_Nishina scatter equation and compare Klein\_Nishina scatter estimation with triple energy window. In order to verify the proposed scattering model several cylindrical phantoms were simulated. The linear source in the cylindrical Phantoms was a hot rod filled with <sup>99m</sup>Tc. K factor defines as the ratio of scatter resulting from MC simulation to scatter estimated from Klein\_Nishina formula. Also a SPECT/CT scan of the image quality phantom was acquired. Row data were transferred to a PC computer for scatter estimation & processing of the images using MLEM iterative algorithm in MATLAB software.

**Results:** The scatter and attenuation compensated images by the proposed model had better contrast than uncorrected and only attenuation corrected images. The K-factors that used in proposed model doesn't vary with different activities & diameters of linear source and they're just a function of depth and composition of pixels.

**Conclusion:** Based on Monte Carlo simulation data, the K\_N formula that used in this study demonstrates better estimation of scattered photons than TEW. Proposed scattered correction algorithm will improve 52.3% in the contrast of the attenuated corrected images of image quality phantom.

**Key words:** Scatter correction; Klein\_Nishina; Nuclear medicine images; Monte Carlo simulation

**Iran J Nucl Med 2013;21(1):19-25**

Published: June, 2013

<http://irjnm.tums.ac.ir>

**Corresponding author:** Shabnam Oloomi, Medical Physics Department, Mashhad University of Medical Science, Mashhad, Iran.  
E-mail: [shabnamolumi@gmail.com](mailto:shabnamolumi@gmail.com)

## INTRODUCTION

The presence of scattered photons in single photon emission computed tomography (SPECT) projection data causes reduction of the contrast and a loss of quantitative accuracy in reconstructed images [1-3]. Numbers of methods have been proposed to compensate the effects of scatter [4-11], many of them estimate and subtract the scattered component of the data such as dual and triple energy window. Such removal of scattered photons leads to increase statistical noise in the image, causing degradation and may outweigh the benefits of performing the scatter correction [12-14]. Alternative scatter correction methods are to correct the scattered photon based on modeling the scatter distribution. In these methods compensation is achieved, in effect, by mapping scattered photons back to their point of origin. Since all of acquired counts are used, the noise increase found with scatter subtraction methods is avoided. The accuracy of these methods depends upon the accuracy of the scatter model used, and such developed models can provide accurate three-dimensional (3-D) scatter compensation in SPECT [15-18].

In this work we introduce MLEM analytical scatter compensation model based on Klein\_Nishina scatter equation [19], to achieve in SPECT images. The K and K' factor are defined for converting the K-N and TEW scatter estimation to MC simulated phantom projection data.

The estimation of scattered photons with the Klein\_Nishina formula is compared with TEW as a routine subtraction technique for scatter correction.

Finally the contrast improvement, from an image quality phantom resulting from proposed algorithm compares with attenuated corrected image is shown.

## METHODS

### Monte Carlo Simulation

In order to verify the proposed scattering model a simulated phantoms with uniform attenuation media was established in SimSET software [20]. Simulated phantom, Figure 1, was a cylinder with 50 cm inner diameter and 30 cm height, containing a  $^{99m}\text{Tc}$  line source, 30 cm long at 20 cm from the center. The projection data was acquired when the cylinder axis was parallel to the bed and the phantom was filled with water. Each phantom was simulated 6 times with different line source diameters, 0.2, 1 and 4.8 cm and different activities, 10 and 40mCi, as the low and high activity used in clinic. These simulated phantoms provided an extended scattering medium and remained simple enough to expedite the analysis process.

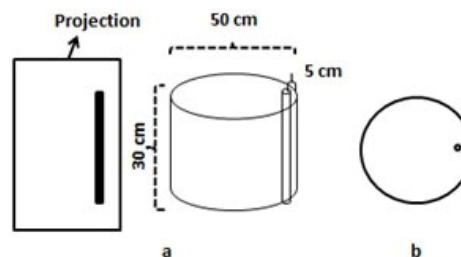


Fig 1. a) Simulated phantom & projection, b) transverse view of phantom.

Four orders of Compton scattering was simulated and large number of photon histories were traced to create essentially low noise data. The projection data were acquired with gamma camera specifications (image size: 64×64, projection No.: 64 over 360°).

The effects of attenuation and scatter were included and data were binned into three energy windows: window1 as photo peak at 126-154 keV, Window 2 at 154-156 keV and Window3 at 92-125 keV. The primary and scatter components of the projection data were stored separately to enable verification of the scatter compensation methods described.

### Phantom study

A SPET/CT scanner, GE Infinia Hawkeye, was used to acquire projection data of an image quality phantom [21], containing 4 hot spheres, 2 holes as cold spheres and an absorber in the center [22]. The background and 4 hot spheres of the phantom were filled with Tc-99m, with an activity concentration ratio of 1:8, the cold spheres activity are zero (Figure 2). Projection data were measured with 64×64 pixels, from 0-360° with 6 degree increments and stored with CT images of the phantom in DICOM format.

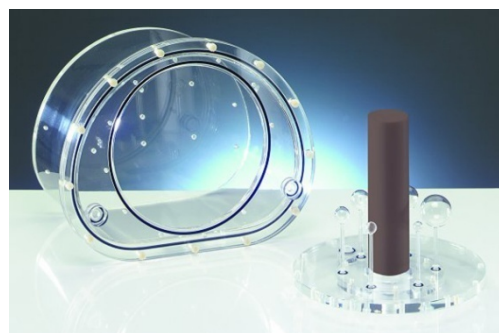


Fig 2. Image quality phantom.

### Proposed algorithm for scatter correction

As scattered photons can be measured precisely by Monte Carlo, the estimated scatter from Klein\_Nishina formula and that measured from

standard Triple Energy Window (TEW) method were first converted to Monte Carlo via K and K' factors and then compared the scatter estimation based on Klein\_Nishina(K\_N) equation with TEW method.

K and K' factors are defined as:

$$K = \frac{\text{scattering measured from Monte Carlo}}{\text{scatter estimated by K\_N formula}}$$

$$K' = \frac{\text{scattering measured from Monte Carlo}}{\text{scatter estimated by TEW}}$$

As scattering seems to be dependent on source size, depth, composition of the medium and activity of the source, K factor were measured on flowing steps:

**Step 1)** to assess the effect of source size on the K factor, the K factor for different line source diameters 0.2, 1 and 4.8cm were measured within same attenuation media.

**Step 2)** to study the dependency of K factor to depths, the data of different projections which resembles the line source at different depths from the surface of the cylinder (5 to 45 cm) were measured.

**Step 3)** to study the dependency of K factor with object composition the simulated phantom were filled with water, lung and bone respectively and measured.

**Step 4)** to assess the effect of activity concentration, different activity 10 and 40mCi were injected into the line source and measured.

Finally k and K', which are obtained through simulation study, can be used in later experimental studies. It means that "K×scatter estimated by K\_N formula" or "K×scatter estimated by TEW" will generate scatter photon counts that are close to scatter photons resulting from Monte Carlo simulation.

#### Scatter estimation method based on K\_N equation

Numbers of authors have published descriptions of analytical equations that allow an exact calculation of scatter photons. These are quite complex, incorporating transport of photons from source to detector with probability of Compton interaction at any point [23-25]. Some of them have used differential cross section ( $d\sigma/d\Omega$ ) of photons scattered from a single free electron as a function of scattering angle ( $\theta$ ) proposed by K\_N formula as follow to build appropriate scatter models for scatter correction in emission tomography.

$$\frac{d\sigma}{d\Omega} = \frac{1}{2} r_e^2 P^2(E_\gamma, \theta) \left( \frac{1}{P(E_\gamma, \theta)^{+P(E_\gamma, \theta) - 1 + \cos(\theta)^2}} \right)$$

Equation 1

Where  $P(E_\gamma, \theta) = \frac{1}{1 + \frac{E_\gamma}{m_e c^2} (1 - \cos \theta)}$  and  $r_e$  is classic

electron radius,  $E_\gamma$  is the incident photon energy and  $P(E_\gamma, \theta)$  is the ratio of photon energy after and before collision. In this paper we would present a mathematical scatter correction approach basis on K\_N scatter equation. In this algorithm according to Equation 2, scattering contributions of each voxels along the detector ( $SC_j$ ) are calculated from emission photons of 26 neighbor voxels in 3 slices (8 in the slice that voxel j belongs to, 9 in the above and 9 in the below slices) using K\_N formula. The scattering photons are then summed for all voxels along each detector in a projection to form a scattered data bin,  $SC_j$  to be used in image reconstruction process. These data can be used in all iterations in the MLEM image reconstruction process.

$$SC_j = \sum_{j-1}^{j+1} \sum_{c-1}^{c+1} \sum_{s-1}^{s+1} K_{j,c,s} \times (K\_N)_{j,c,s} \times f_{j,c,s}$$

Equation 2

Where pixel j belongs to slice s and column c, K is the aforementioned factor that corrects the Klein\_Nishina scatter estimation to Monte Carlo data,  $K\_N$  is the Klein-Nishina scatter count and f is the count of pixel j.

#### Scatter estimation based on TEW method

The TEW approach relies on relatively narrow energy windows placed close on either side of the photo-peak [9]. The scattering photons for each pixel,  $C_{scat}$ , can be calculated from the following equation:

$$C_{scat} \cong \left( \frac{C_{left}}{W_s} + \frac{C_{right}}{W_s} \right) \frac{W_m}{2}$$

Equation 3

Where  $W_m$  and  $W_s$  are photo peak and narrow energy window widths,  $C_{right}$  and  $C_{left}$  are the counts on left and right windows, respectively. The selection of scatter windows close to the photo-peak aims to achieve good estimation of the scatter distribution while providing a realistic estimate of the scatter fraction. This approach involves subtraction of the scatter estimate, pixel by pixel, from the photo-peak projection data.

#### Image Reconstructions

A conventional MLEM formula was used for image reconstruction algorithm as no correction images [26].

It is used with  $a_{ij}(\mu) = a_{ij} * e^{-\sum_{k \in k_{i,j}}^m r_{ik} \mu_k}$  to reconstruct attenuation corrected images, which  $r_{ik}$  and  $\mu_k$  are respectively the length and attenuation coefficient of pixel  $k$ , which is along the direction of pixel  $j$  to detection bin  $i$ . It should be mentioned that GE Infinia Hawkeye system used bilinear energy mapping to convert CT numbers to attenuation coefficients of  $^{99m}\text{Tc}$  [27-29]. Equation 4 was used for attenuation and scatter corrected images.

$$f_j^{p+1} = \frac{f_j^p}{\sum_{i=1}^n a_{i,j}} \sum_{i=1}^n \frac{g_i}{\sum_{l=1}^m a_{i,l} f_l^p + SC_i}$$

$i = 1, 2, 3, \dots, n$  &  $j = 1, 2, 3, \dots, m$

Equation 4

Where  $f_j^p$  represents pixel value of the image in  $p^{\text{th}}$  iteration,  $g_i$  the measured SPECT emission data,  $a_{i,j}$  the elements of the system matrix,  $SC_i$  the scatter estimation, which is equal to sum of  $SC_j$  along the direction of detection bin  $i$  at  $p^{\text{th}}$  iteration.

In equation 4, attenuation and scatter correction were performed using  $\mu$ -values from CT data of image quality phantom as an attenuation map and the proposed algorithm for scatter compensation.

To assess the effect of attenuation and scatter corrections, image contrast improvement was measured using the difference of mean target and mean background that divided by mean background of predefined ROIs. The target ROI and background ROI were selected as 3 pixels around a hot spot and 7 pixels of background through the profile.

## RESULTS AND DISCUSSION

Depth dependence of K-factor to different object composition is shown on Figure 3.

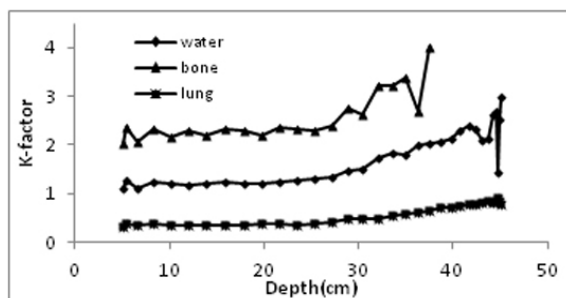


Fig 3. Variation of K-factor with depth in different medium, for 0.2 cm diameter line source; 10 mCi activity.

This figure shows that variation of K-factors for 0.2 cm diameter line source and 10 mCi activities keeps the same trends in water, bone and lung. They are

increased slowly with depth especially near the sources (up to 30 cm), and is nearly close to 1 for water, which means that the K\_N formula estimate the scattering photons close to true scattering by Monte Carlo. For lung and bone those values are lower and higher meaning that the scattering will be over and under estimate respectively by K\_N.

To assess the effect of source size, different line source diameters with constant specific activity of 0.094 mCi/cm<sup>3</sup> were studied. Results in water phantom are shown in Figure 4.

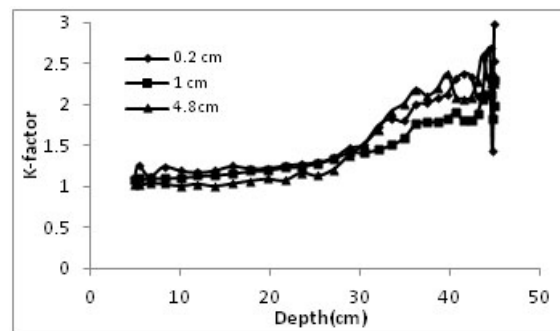


Fig 4. Variation of K-factor with depth in water phantom, for different line source diameter and constant specific activity of 0.094 mCi/cm<sup>3</sup>.

In order to assess the significance of differences, a one-way ANOVA was performed on the K-factor by categorizing the source sizes. Note that the  $p$ -values for the  $F$  statistic are lower than a 0.01 significance level. However, no significant differences in K-factors were found between 0.2, 1 and 4.8 cm line sources (e.g.  $P$ -value=0.095 between sources of 0.2 and 1 cm diameter). Activity dependence of K factor was studied with different amounts of activity (10 and 40 mCi as the lowest and highest activity used in clinic) injected into the line source. The results show no significant difference for K factors with different activities (Figure 5).

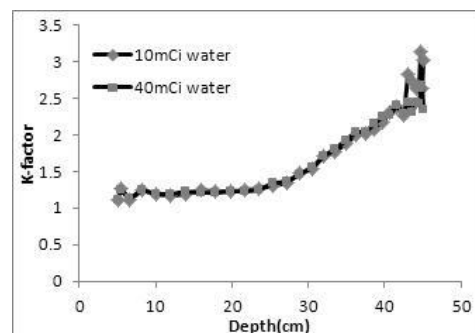


Fig 5. Variation of K factor with depth, for different activity.

Figures 4 and 5 show that variation of K factor with depth is independent of source size and activity. So in equation 2, K for each pixel is a function of depth and composition of that pixel. The rapid variation of K\_factor after 30 cm depth in Figures 4, 5 and 6 caused by low counts of related projections and therefore small signal to noise ratio.

To compare the capability of K\_N to estimate the scatter photons with respect to TEW, variation of K'/K factors with depth for different medium were calculate and shown in Figure 6. The results showed that except for bone phantom that k and k' are nearly the same, in other media K' is higher than K which means TEW estimate the scattering photons less than proposed K\_N algorithm.

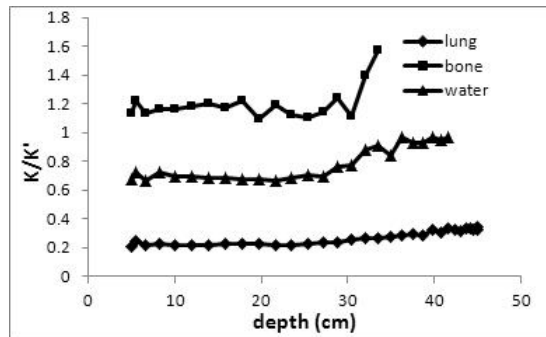


Fig 6. Variation of K/K' with depth, for different medium.

In the authors point of view it can cause by difference in the scatter estimation based on TEW and K\_N. In TEW method, only the below subwindow counts were used to estimate scatter counts in the photopeak window, in other words, as the energy of photon (channel) increase in the photopeak, the proportion of scattered counts decrease in that channel according to the triangular approximation, but in K\_N method the proportion of scatter photons in different energy channel changed according to special equation which is not a linear approximation, so the scatter estimation based on K\_N was bigger than TEW scatter estimation.

Figure 7 illustrates the 42<sup>th</sup> slice of image quality phantom, that reconstructed with no correction (Figure 7a), with attenuation correction (Figure 7b) and with scatter and attenuation correction through the proposed algorithm (Figure 7c). In all cases 10 iterations of MLEM formula are used. The results are shown in Figure 7 and represents:

1: non-uniformity of the photons at the center of uncorrected image, (Figure 7a) (more photons near edge than center) has been changed to uniform using attenuation correction (Figure 7b).

2: the spared uniform scattered photons on the image 7b have also been removed using proposed scatter correction algorithm (Figure 7c).

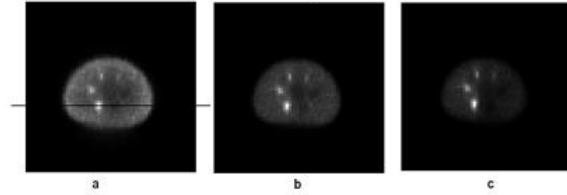


Fig 7. Reconstructed slice of the image quality phantom with 10 iteration, a: with no correction, b: attenuation corrected, c: attenuation and scattered corrected.

The performance of attenuation and scatter correction via proposed method was also evaluated by the horizontal profile through a hot spot as shown on Figure 7a. Attenuation correction increased the values of the uncorrected profile while scatter and attenuation correction via proposed model decreased the values from attenuated corrected profile (Figure 8).

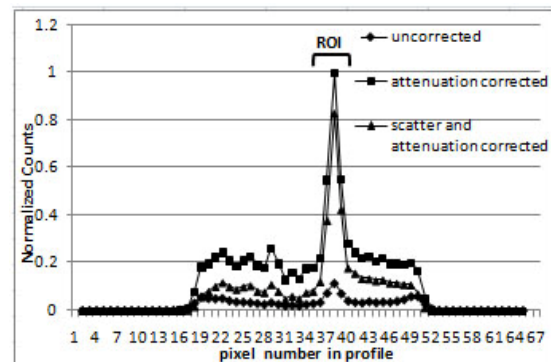


Fig 8. Selected profile of the image through hot spot, ROI is pixels 35:37.

In Figure 8, Contrast value in uncorrected, attenuation, attenuation and scatter corrected images are 0.84, 1.95 and 2.97, respectively. That means only attenuation correction will improve the contrast by 132% and attenuation with scatter correction by 153%. In other word the proposed scatter correction method will improve 52.3% in the contrast of attenuated corrected images.

The scatter and attenuation compensated images had better contrast than the uncorrected images, so the lesions were better defined in the scatter and attenuation-compensated images. This is in agreement with the trials demonstrated that scatter & attenuation can increase contrast in SPECT studies [30].



## CONCLUSION

Based on the Mont Carlo simulation data as a standard method for estimation of scattered photons, the  $K_N$  formula that used in this study demonstrates better estimation of scattered photons than TEW to be used in image reconstruction.

Proposed scattered correction algorithm can be used successfully in clinical images. It is quite fast and effectively corrects the scattered photons.

Proposed scattered correction algorithm will improve 52.3% in contrast of the attenuated corrected images.

## Acknowledgements

We would like to thank from research vice-president of Mashhad University of Medical Sciences for the financial supports and appreciate the manager of Nuclear Medicine Department of Wilhelminenspital Vienna for their kind collaborations.

## REFERENCES

- Blundell HL, Middleton GW, Lee AJ, Tweddel AC. The impact of scatter correction of SPECT myocardial perfusion images on the clinical report. *Nucl Med Commun.* 2001;22(4):434.
- Kangasmaa TS, Kuikka JT, Vanninen EJ, Mussalo HM, Laitinen TP, Sohlberg AO. Half-time myocardial perfusion SPECT imaging with attenuation and Monte Carlo-based scatter correction. *Nucl Med Commun.* 2011 Nov;32(11):1040-5.
- Ali L, Khalil M, Muddei S, Burezq S, Al-Hajri B. Ga-67 scintigraphic imaging: role of combined optimized energy photopeaks and scatter correction in improving lesion detectability. *Nucl Med Commun.* 2011 Aug;32(8):724-30.
- Hutton BF, Buvat I, Beekman FJ. Review and current status of SPECT scatter correction. *Phys Med Biol.* 2011 Jul 21;56(14):R85-112.
- King MA, Hademenos GJ, Glick SJ. A dual-photopeak window method for scatter correction. *J Nucl Med.* 1992 Apr;33(4):605-12.
- Floyd CE Jr, Jaszczak RJ, Greer KL, Coleman RE. Deconvolution of Compton scatter in SPECT. *J Nucl Med.* 1985 Apr;26(4):403-8.
- Meikle SR, Hutton BF, Bailey DL. A transmission-dependent method for scatter correction in SPECT. *J Nucl Med.* 1994 Feb;35(2):360-7.
- Narita Y, Eberl S, Iida H, Hutton BF, Braun M, Nakamura T, Bautovich G. Monte Carlo and experimental evaluation of accuracy and noise properties of two scatter correction methods for SPECT. *Phys Med Biol.* 1996 Nov;41(11):2481-96.
- Ogawa K, Harata Y, Ichihara T, Kubo A, Hashimoto S. A practical method for position-dependent Compton-scatter correction in single photon emission CT. *IEEE Trans Med Imaging.* 1991;10(3):408-12.
- Koral KF, Wang XQ, Rogers WL, Clinthorne NH, Wang XH. SPECT Compton-scattering correction by analysis of energy spectra. *J Nucl Med.* 1988 Feb;29(2):195-202.
- Pretorius PH, van Rensburg AJ, van Aswegen A, Lötter MG, Serfontein DE, Herbst CP. The channel ratio method of scatter correction for radionuclide image quantitation. *J Nucl Med.* 1993 Feb;34(2):330-5.
- de Vries DJ, King MA, Soares EJ, Tsui BMW, Metz, CE. Evaluation of the effect of scatter correction on lesion detection in hepatic SPECT imaging. *IEEE Trans Nucl Sci.* 1997;44(5):1733-40.
- Larsson A, Johansson L, Sundström T, Ahlström KR. A method for attenuation and scatter correction of brain SPECT based on computed tomography images. *Nucl Med Commun.* 2003 Apr;24(4):411-20.
- Lagerburg V, de Nijs R, Holm S, Svarer C. A comparison of different energy window subtraction methods to correct for scatter and downscatter in I-123 SPECT imaging. *Nucl Med Commun.* 2012 Jul;33(7):708-18.
- Frey EC, Tsui BMW. A practical method for incorporating scatter in a projector-backprojector for accurate scatter compensation in SPECT. *IEEE Trans Nucl Sci.* 1993;40(4):1107-16.
- Frey EC, Ju ZW, Tsui BMW. A fast projector-backprojector pair modeling the asymmetric, spatially varying scatter response function for scatter compensation in SPECT imaging. *IEEE Trans Nucl Sci.* 1993;40(4):1192-97.
- Beekman FJ, Eijkman EGJ, Viergever MA, Borm GF, Slijpen ETP. Object shape dependent PSF model for SPECT imaging. *IEEE Trans Nucl Sci.* 1993;40(1):31-39.
- Frey EC, Tsui BMW. A new method for modeling the spatially-variant, object-dependent scatter response function in SPECT. *IEEE Nucl Sci Symp Med Imaging Conf.* 1996;2:1082-86.
- Klein-Nishina formula. [[http://en.wikipedia.org/wiki/Klein%E2%80%93Nishina\\_formula](http://en.wikipedia.org/wiki/Klein%E2%80%93Nishina_formula)].
- Harrison R. SimSET. [[http://depts.washington.edu/simset/html/simset\\_main.html](http://depts.washington.edu/simset/html/simset_main.html)].
- PET Emission Phantom acc NEMA NU2-2007. [[http://www.ptw.de/pet\\_emission\\_phantom\\_nema.html](http://www.ptw.de/pet_emission_phantom_nema.html)].
- Knoll P, Kotalova D, Köchle G, Kuzelka I, Minear G, Mirzaei S, Sámal M, Zadrzil L, Bergmann H. Comparison of advanced iterative reconstruction methods for SPECT/CT. *Z Med Phys.* 2012 Feb;22(1):58-69.
- Riauka TA, Gortel ZW. Photon propagation and detection in single-photon emission computed tomography--an analytical approach. *Med Phys.* 1994 Aug;21(8):1311-21.
- Riauka TA, Hooper HR, Gortel ZW. Experimental and numerical investigation of the 3D SPECT photon detection kernel for non-uniform attenuating media. *Phys Med Biol.* 1996 Jul;41(7):1167-89.
- Wells RG, Celler A, Harrop R. Analytical calculation of photon distributions in SPECT projections. *IEEE Trans Nucl Sci.* 1998;45(6):3202-14.

26. de Waard JC. Image reconstruction methods for emission based tomography. Master thesis. Faculty of Science, Utrecht University; 2011.
27. Seo Y, Wong KH, Sun M, Franc BL, Hawkins RA, Hasegawa BH. Correction of photon attenuation and collimator response for a body-contouring SPECT/CT imaging system. *J Nucl Med.* 2005 May;46(5):868-77.
28. Teimourian B, Ay MR, Zafarghandi MS, Ghafarian P, Ghadiri H, Zaidi H. A novel energy mapping approach for CT-based attenuation correction in PET. *Med Phys.* 2012 Apr;39(4):2078-89.
29. Kheruka S, Naithani U, Maurya A, Painuly N, Aggarwal L, Gambhir S. A study to improve the image quality in low-dose computed tomography (SPECT) using filtration. *Indian J Nucl Med.* 2011 Jan;26(1):14-21.
30. Kalantari F, Rajabi H, Saghari M. Quantification and reduction of attenuation related artifacts in SPET by applying attenuation model during iterative image reconstruction: a Monte Carlo study. *Hell J Nucl Med.* 2011 Sep-Dec;14(3):278-83.